Proceedings of
11th European Conference on Turbomachinery Fluid dynamics & Thermodynamics
ETC11, March 23-27, 2015, Madrid, Spain

ANALYSING NON-SYNCHRONOUS BLADE VIBRATIONS IN A TRANSONIC COMPRESSOR ROTOR

M. Jüngst - F. Holzinger - H.-P. Schiffer

Technische Universität Darmstadt
Institute of Gas Turbines and Aerospace Propulsion
Otto-Berndt-Straße 2, 64287 Darmstadt, Germany

S. Leichtfuss

Turbo Science
www.turboscience.de
64287 Darmstadt, Germany

ABSTRACT

This paper aims to add to the understanding of non-synchronous blade vibration caused by unsteady flow close to the stability limit of transonic compressor rotors. Blade vibrations are measured in the rotating frame of reference by strain gauges applied to the blades and additionally in the stationary frame of reference by capacitive tip clearance/tip timing sensors. Furthermore unsteady pressure transducers in the casing wall are used to analyse the flow phenomena during high blade vibration amplitudes. During the transient experiments, the compressor is back-pressured into its stability limit. Two transient measurements of a compressor setup with an enlarged tip clearance of 2.5% blade chord are analysed at part speed and design speed. This means that subsonic and transonic operation conditions are analysed. In both cases, non-synchronous vibration occurred and limited the compressor operation. The mechanism leading to these vibrations is based on an unsteady flow pattern that rotates relative to the rotor, reported as rotating instability.

NOMENCLATURE

ADP	Aerodynamic Design Point	VIGV	Variable-Inlet-Guide-Vanes
AR	Amplitude Rise	$A_{max}(\Delta f)$	Maximum Amplitude in a Range of Frequencies
BPF	Blade Passing Frequency	C	Chord Length
BTC	Blade Tip Clearance	f	Frequency
BTT	Blade Tip Timing	F^+	Reduced Frequency
EO	Engine Order	N	Number of Ensembles
LE	Leading Edge	p_s	Static Pressure
ND	Nodal Diameter	p_t	Total Pressure
PS	Pressure Side	U_∞	Reference Flow Velocity Upstream Rotor LE
SS	Suction Side	U_{tip}	Blade Tip Speed
RI	Rotating Instability	Π	Pressure Ratio
SG	Strain Gauge	ρ	Density
TE	Trailing Edge	σ_{rel}	Relative Standard Deviation
TO	Throttle Opening	Ψ	Total-to-Static Pressure Rise Coefficient

INTRODUCTION

Modern compressor rotor designs are more vulnerable to blade vibration due to minimal structural damping. This emerged as a result of higher stage loading, thinner blades and blade integrated disk designs (BLISK). Therefore, more research is needed to understand the different mechanisms leading to aeroelastic and aerodynamic phenomena close to the compressor operation limits in state-of-the-art compressors. The 1.5-stage Darmstadt Transonic Compressor was designed to investigate aerodynamic and aeroelastic behaviour. For the current investigation a modern BLISK rotor is chosen.

In general, the vibrations of rotors are distinguished by being synchronous or non-synchronous. Syn-

chronous vibrations are a result of a steady flow field, which is varying in circumferential direction. E.g. these variations belong to stator wakes or potential fields. Since the mechanisms leading to synchronous vibrations are generally understood, research is focusing on vibrations which occur at non integer multiples of the rotor speed. Besides the historically well known term *flutter*, the more general term *non-synchronous vibrations* (NSV) has been subject to several publications during the past two decades (Kielb et al. [2003], Vo [2006], Martensson et al. [2012], Andersson et al. [2013]).
Flutter is characterized as a self-excited vibration that stops when the motion of the blade stops and therefore as a stability problem (Sisto [1988]).
The term NSV is commonly used for vibrations caused by pressure fluctuations locking-on to a blade mode if the frequency of the fluid dynamic instability matches the eigenfrequency of a rotor blade. This can result in high amplitude excitations. The description implies that a flow phenomenon can occur, even though it is not locked-on to an eigenfrequency of the blades. One such flow phenomenon, which is known as *rotating instability* (RI), is widely investigated, since it is identified being a driving mechanism for NSV and also being a source of noise.
A characteristic frequency pattern in the casing wall pressure of a multi-stage high-speed axial compressor was reported by Baumgartner et al. [1995]. A theoretical model was presented to explain the characteristic frequency pattern in the casing wall pressure. The phenomenon was identified to be a pressure fluctuation that rotates around the compressor duct exciting mechanical modes to high amplitudes.
The investigations of Mailach et al. [2001a] and Mailach et al. [2001b] basically showed, that the blade tip clearance flow interacts periodically and that there is a fluctuating blade tip vortex trajectory angle. Furthermore, a region with reversed axial flow was observed and shifted upstream when approaching the stability limit. An analysis of the pressure difference between pressure side and suction side of a blade indicated that the tip clearance flow is periodically stopped or even reversed. The observed RI was moving with a circumferential velocity of about 50 to 60% of the rotor velocity.
Numerical and experimental investigations of the RI were performed by März et al. [2002]. The detailed analysis of the tip clearance flow showed a vortex moving from the suction side of the passage to pressure side of the adjacent blade. Unsteady calculations of the full annulus indicated a blockage and axially reversed flow during RI conditions.
An experimental study of the periodic unsteadiness of the compressor tip vortex was presented by Bae et al. [2004]. The observed reduced frequencies of the tip clearance vortex fluctuation lie between 0.6 and 1.0 (calculated using the frequency of the pressure fluctuations, chord length of the blades and cascade inlet flow velocity). The reduced frequency drops when moving downstream in the passage. Additionally an analytical model was developed to explain the observed frequency range. It was found that the time scale of the vortex instability is that of the convective time through the pitch.
Kameier and Neise [1997] showed by a tip gap size variation, that compressors with larger tip gaps tend to build up RI. A significant sound pressure level increase is reported for tip clearance ratios larger than 2.8% blade tip chord. Mailach et al. [2001b] investigated tip gap sizes of 1.3% to 4.3% and observed RIs for tip gaps larger than 3%. Kielb et al. [2003] report NSV due to a fluid dynamic instability in the first stage of a compressor rotor using a setup with a tip gap of 1.1% blade tip chord. For the measurements, presented in this paper, an enlarged tip gap of 2.5% blade tip chord is applied to the rotor section of the compressor. As a result of the large tip gap high blade amplitudes are observed, which limit the compressor operation. These are characterized and analysed in detail in this paper. The following objectives are the starting point of this investigation:

1. Data analysis of transient measurements close to the stability limit of a modern transonic compressor rotor
2. Characterization of the observed phenomena
3. Further insight into the unsteady flow field and understanding of the underlying vibration mechanism

RESEARCH FACILITY AND INSTRUMENTATION

In this section the *TU Darmstadt* compressor research facility and the instrumentation is introduced.

Key characteristics	
power	800 kW DC
design mass flow	16 kg/s
max. shaft speed	21,000 rpm
max. shaft torque	350 Nm
max. pressure ratio	1.6
inflow/outflow	axial/axial

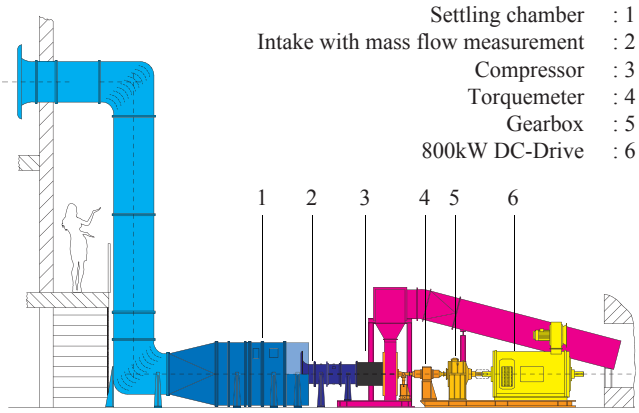

Figure 1: Research facility of the Darmstadt Transonic Compressor

Research Facility Figure 1 illustrates the compressor research facility. The test rig is driven by an 800 kW DC drive. A gearbox enables the test rig to run up to 21,000 rpm maximum shaft speed and 350 Nm maximum shaft torque, measured with a torquemeter. The rig is run in an open cycle, taking air from ambient conditions. The incoming flow enters the test rig through a settling chamber and the intake, after which the mass flow is determined. The transonic compressor is run as a 1.5-stage compressor with Variable-Inlet-Guide-Vanes (VIGV). VIGV and stator can be clocked for performance measurements. After the flow has passed the actual test section, the air is guided by a radial diffuser to the throttle and from there back into ambience. The outlet cavity is comparably small and thus a stalled rotor will not lead to compressor surge. This can be perfectly used for transient experiments at the compressor stall line.
The rig is greatly instrumented for performance measurements, which is described in detail by Biela [2012]. In the following section the unsteady instrumentation during the performed measurement campaign is presented.

Unsteady Instrumentation An overview of the unsteady instrumentation is given in Figure 2. Figure 2a shows the circumferential distributed sensors and Figure 2b illustrates the axial array of the pressure transducers. Blade vibrations are measured in the rotating frame of reference with strain gauges (SG) applied to the blades and additionally in the stationary frame of reference by capacitive tip clearance/tip timing (BTC/BTT) sensors (Fogale nanotech MCC5-20T). By comparing the measured frequency of both, the nodal diameter (ND) and thus the inter blade phase angle can be determined. Consequently, the whole BLISK vibration pattern is investigated, using the SG and BTT instrumentation.
The same frequency shift is of course observed when comparing frequencies of the SG instrumentation and unsteady pressure transducers in the casing wall. These pressure transducers (Kulite XCS-062) are used to analyse the flow phenomena during high blade vibration amplitudes. They are clustered in axial and circumferentially distributed arrays. The Kulites are sampled with a frequency of 500 kHz. However, the eigenfrequency of these pressure transducers lies at about 150 kHz. A low pass filtering is therefore applied at 100 kHz.
The axial array can be used to resolve the unsteady pressure field at the casing wall. Its spatial resolution is illustrated in Figure 2b. Since the blades pass the stationary axial array during their rotation

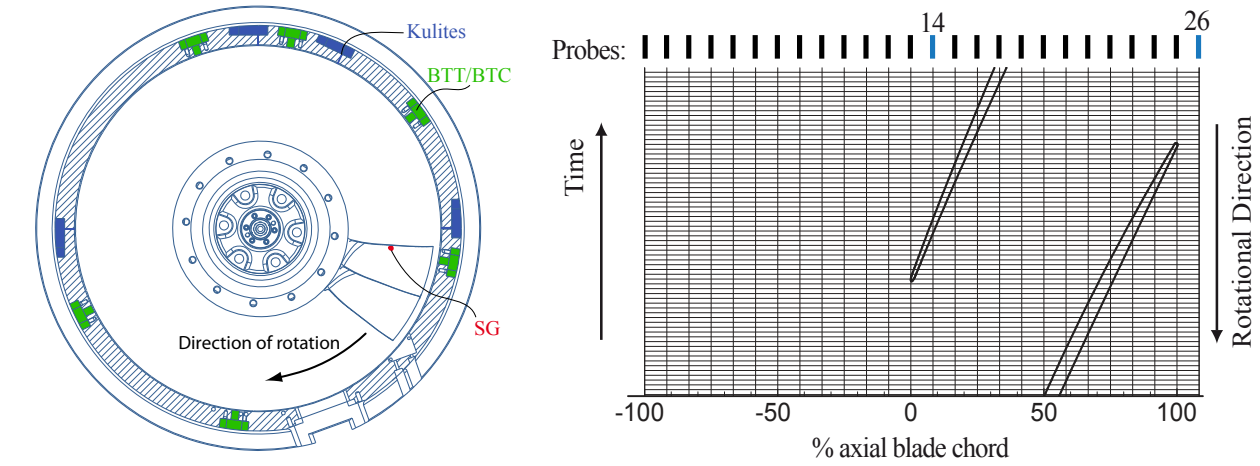

(a) Circumferential distributed instrumentation

(b) Spatial resolution of the axial Kulite array

Figure 2: Unsteady instrumentation

around the annulus, the circumferential resolution is a function of the rotor speed. At 80% rotor speed one passage is resolved with approximately 90 measurements. The axial resolution is simply given by the distance between two Kulite sensors in the casing. During the presented measurements, 26 sensors are used which leads to a axial resolution of 8% axial blade chord length. The array spans from 100% axial blade chord upstream of the leading edge (LE) to 108% downstream. Thereby the shock and all major flow features in the rotor section are captured.

COMPRESSOR MAP AND MEASUREMENT PROCEDURE

The steady measurements with the enlarged tip gap setup are presented in Figure 3 and compared to the performance of the reference case. The steadily measured operation points are illustrated with triangle markers.

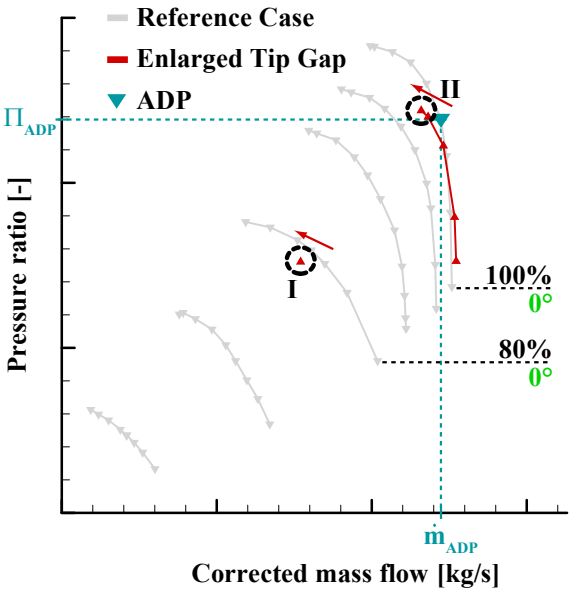

Figure 3: Compressor Map

As one would expect, the maximum reachable pressure ratio is lower for the enlarged tip gap, since the losses become more severe as the tip clearance increases. Hence, the stability limit is shifted to higher mass flows. For further illustration the aerodynamic design point (ADP) is shown.

Two transient measurements close to the stability limit are investigated in detail in the following sections. Measurement I is performed at 80% aerodynamic speed which leads to subsonic operation conditions with relative rotor inlet Mach number close to 1. During measurement (II) the compressor is driven at transonic operation conditions with 100% aerodynamic speed. These transient measurements are performed with a VIGV angle of 0°.

For the measurements, the compressor is continuously back-pressured into its stability limit (Figure 3: marked with red arrows), starting at the last stable point of a speed line (Figure 3: marked with black dashed circles). The throttle is closed until the aero-

dynamic or aeroelastic stability limit is reached, which means that stall or high amplitude blade vibrations occur. In case of stall the pressure ratio across the rotor drops. By contrast, the pressure ratio does not necessarily drop when aeroelastic phenomena limit the compressor operating range. However the high blade amplitudes limit the compressor operation. To avoid damaging of the compressor the back-pressure has to be reduced rapidly by an emergency bleed in the throttle in both cases.

DATA ANALYSIS

Blade Mode and BLISK Vibration Analysis To analyse the active blade modes during the performed measurements the blade mounted SG are used. In addition, to picture the vibration pattern of the whole BLISK, the SG and BTT data are combined.

In Figure 4 the SG and BTT amplitudes during Measurement I are plotted against revolution and engine order, whereby the revolutions represent the passing time of the measurements respectively.

For the computation of the shown spectrogram a short-time Fourier transformation is used[1].

The measurement starts at revolution 0 and from left to right the throttle is continuously closed to further back-pressure the rotor into stability limit. At approximately revolution 1400 the back-pressure is reduced rapidly by the throttle opening (TO) which is necessary due to high blade vibrations. During the measurement, shortly before revolution 500, the first amplitude rise (AR) leads to considerable blade amplitudes at non-synchronous vibration conditions (non integer EO). The observed frequencies can be matched to the eigenfrequency of blade mode 4 (see SG spectrogram). This mode is excited to even higher amplitudes at revolution 1050 (second AR), which limit the compressor operation and lead to the final TO. Note that the blade vibrates in a range of approximately 16% of the blades' first eigenfrequency around blade mode 4. This is broadband compared to classical flutter observations as observed by Gill and Capace [2004] or collected by Srinivasan, A. V. [1997]. Besides, parallel lines are visible in the SG spectrogram, which seem to cross blade mode 4 from higher to lower frequencies.

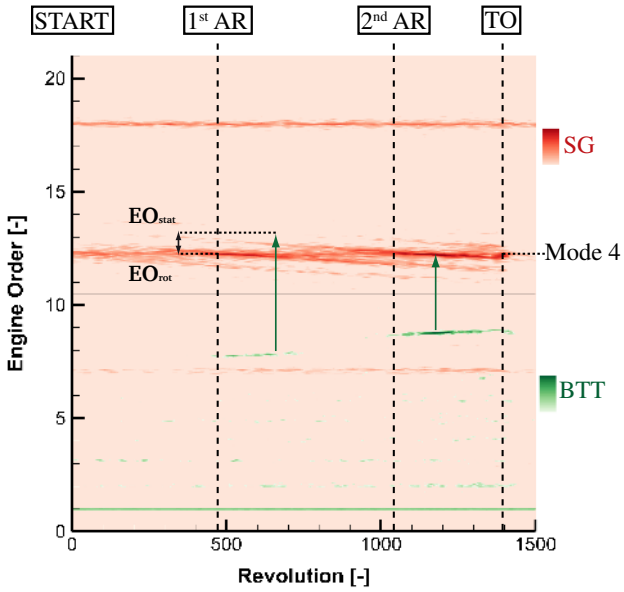

Figure 4: SG and BTT spectrogram (Measurement I)

By comparing the BTT spectrum with the SG spectrum, measurements in the stationary (EO_{stat}) and rotating (EO_{rot}) frame of reference are matched. As a result of the frequency shift between both frames of reference, the nodal diameter can be determined.

Only integer values can be used for the ND to match the frequencies in both frames. This only works out if subsampling effects of the BTT system are taken into consideration for Measurement I. Due to this effect the BTT frequency is mirrored at engine order 10.5. The green arrows in Figure 4 illustrate the frequency shift based on aliasing effects. The effect emerges from the measurement technique itself, since the blades are only detected when passing the sensor (one probe is used around the circumference). The spectrum shown here is called All-Blade-Spectrum. A detailed description of the measurement technique was provided by Zielinski and Ziller [2000]. During the measurement, a change of the ND between the two mode 4 amplitude rises are observed. The ND changes from 1 ND for the first AR at revolution 500 to 0 ND for the second AR.

[1]For one STFT sequence 30 revolutions, a 50% window overlap and a Hanning window is used. This results in a frequency resolution of approximately 8 Hz.

For the transonic Measurement II an analogous SG and BTT analysis is used to determine the limiting blade mode and BLISK vibration. During this measurement, mode 4 amplitudes limit the compressor operation with a change of the ND from 5 to 4 in this case. In the following sections Measurements I and II are analysed side by side.

Characterization of the Observed Phenomena To characterize the observed phenomena in both measurements and to clarify the cause of the blade vibration, insight into the unsteady flow field, knowledge of the blade vibration and the pressure ratio are taken together. Therefore the SG and Kulite instrumentation is used. Represented by the blue line of the upper diagrams in Figure 5, the total-to-static pressure rise coefficient Ψ is visualized. It is calculated using the static pressure of a Kulite sensor located 8% axial chord downstream of TE (see Figure 2b, sensor 26):

$$\Psi = \frac{p_{\mathrm{s},26} - p_{\mathrm{t,inlet}}}{0.5 \rho_{\mathrm{inlet}} U_{\mathrm{tip}}^2} \tag{1}$$

The compressor is continuously back-pressured into its stability limit. Note that the total-to-static pressure rise coefficient is continuously raised and does not reach the maximum pressure rise of the speedline. The final throttle opening is visible by a rapid drop of Ψ.
The blade amplitudes of the monitored blade mode 4 are also shown in the upper diagram. Therefore, the time signal of a particular SG is bandpass filtered to emphasize the content and amplitudes of the signal that belong to blade mode 4. For the filtering a FIR equiripple design with a 300 Hz bandwidth is used.
To keep the blade stresses in acceptable ranges, SG amplitude limits are defined for the modes respectively. These are determined based on high cycle fatigue investigations. During Measurement I the amplitudes of mode 4 reached 20% of the defined limit. In case of Measurement II even higher amplitudes are observed that almost reached 30% of the accepted limit. This illustration of the blade amplitude presents the two amplitude rises that occurred during both measurements. From the BLISK vibration analysis it is known that the ND changes during the measurements between the particular peaks.

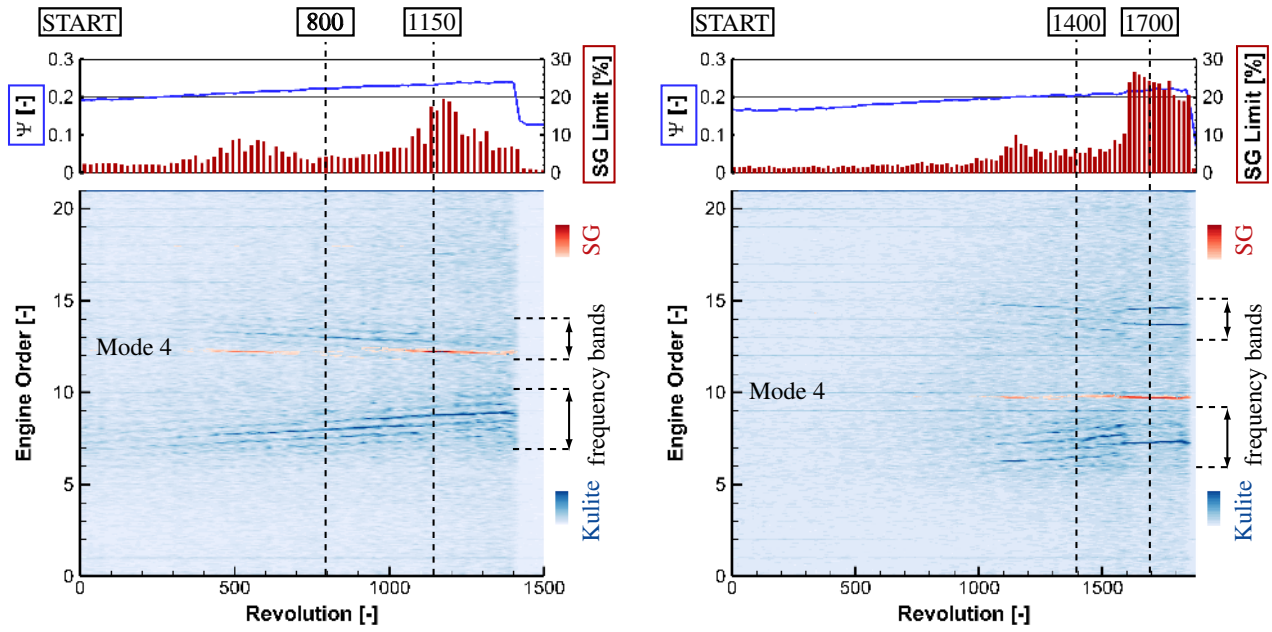

(a) Measurement I: 80% rotor speed, 0° VIGV angle

(b) Measurement II: 100% rotor speed, 0° VIGV angle

Figure 5: Measurement Overview — SG data in red; Kulite data in blue

In Figure 5 the spectrograms of the SG instrumentation and one Kulite sensor are shown in the lower diagram. Therefore, the Kulite sensor of the axial array at 8% downstream of the LE is taken (see Figure 2b, sensor 14). The spectrogram of the pressure transducer obviously shows two frequency bands in both measurements, that belong to a broadband flow structure. During Measurement I its pattern arises at around revolution 400. Likewise it appears in Measurement II, starting close to revolution 1100. The distance of the parallel lines in these frequency bands equals about half of the rotor speed at both operation points and thus $^1/_2$ EO in both cases. This develops from several aerodynamic modes rotating around the annulus with about half of the rotor speed. The theoretical background was given by Baumgartner et al. [1995]. Moreover, the measured frequencies of the pattern are changed continuously due to throttle closing over the whole measurement. This was reported earlier by Kameier and Neise [1997]. These observations lead to the conclusion that the flow structure is a *rotating instability* (RI), which means that pressure fluctuations rotate around the compressor annulus with about 50% rotor speed.
Comparing the amplitude of the RI frequencies to the amplitude of the BPF gives a 10% smaller RI amplitude for the presented cases. The similar scaling was reported by Baumgartner et al. [1995] using a pressure transducer close to the LE of the rotor.
The RI flow structure is also reported by Kameier and Neise [1997] for compressors with a tip clearance larger than 2.8% blade tip chord and by Mailach et al. [2001b] for relative tip gaps larger than 3%. In our case the tip clearance of the enlarged tip gap setup is 2.5%, which is smaller compared to both publications.
Analogously two frequency bands of the RI, that add up to the BPF, are found by Kameier and Neise [1997] and Baumgartner et al. [1995] and in Measurement I and II. In like manner the lower frequency band consists of higher amplitudes. Furthermore the measured frequency of the RI is changed continuously due to throttle closing, but in contrast to Kameier and Neise [1997] the frequencies of the lower band are raised in our case.
In general, Measurement I and II appear to show the same aeroelastic mechanism. As earlier stated by Baumgartner et al. [1995] the pressure fluctuations of the RI can excite the rotor blades to high amplitudes. Under these conditions, the structural and aerodynamic ND are the same. In this paper, blade mode 4 synchronizes with the pressure fluctuations in a range of 16% of the blades' first eigenfrequency. This happens two times during Measurement I and II, enabled by a change of the interblade phase angle (Measurement I: structural ND 1 to 0 / Measurement II: structural ND 5 to 4). Especially during Measurement II a strong fluid-structure interaction appears for the vibration between revolution 1600 and 1890 (mode 4 and ND 4), since all modes of the RI pattern vanish except one which is self-excited when the frequency in the flow locks-on to the blades' eigenfrequency. Thus, not only the pressure fluctuations excite the blade vibrations, additionally the blades reinforce the fluctuations in the flow when frequency and interblade phase angle match structurally and aerodynamically.
Accordingly, the observed phenomenon is a *non-synchronous vibration excited by the rotating instability* and it is thus promising to further investigate different parts of the measurements focusing on the unsteady flow to shed more light on the excitation mechanism.

Flow Study - Unsteady Pressure Field For the investigation of the unsteady flow field, two revolutions are chosen of Measurement I and II respectively. A particular revolution during one measurement can be identified using a once-per-revolution trigger input. Measurement I is analysed at revolution 800 and 1150. During both revolutions the flow is dominated by the RI, exciting the structure at revolution 1150 in contrast to revolution 800. Equivalent, for the transonic Measurement II revolution 1400 and 1700 are chosen for analysis. These revolutions are visualized in Figure 5.
The pressure field is shown from 100% axial chord upstream to 108% downstream in axial direction and about one third of the specified revolution in circumferential direction (Figure 6). The pressure

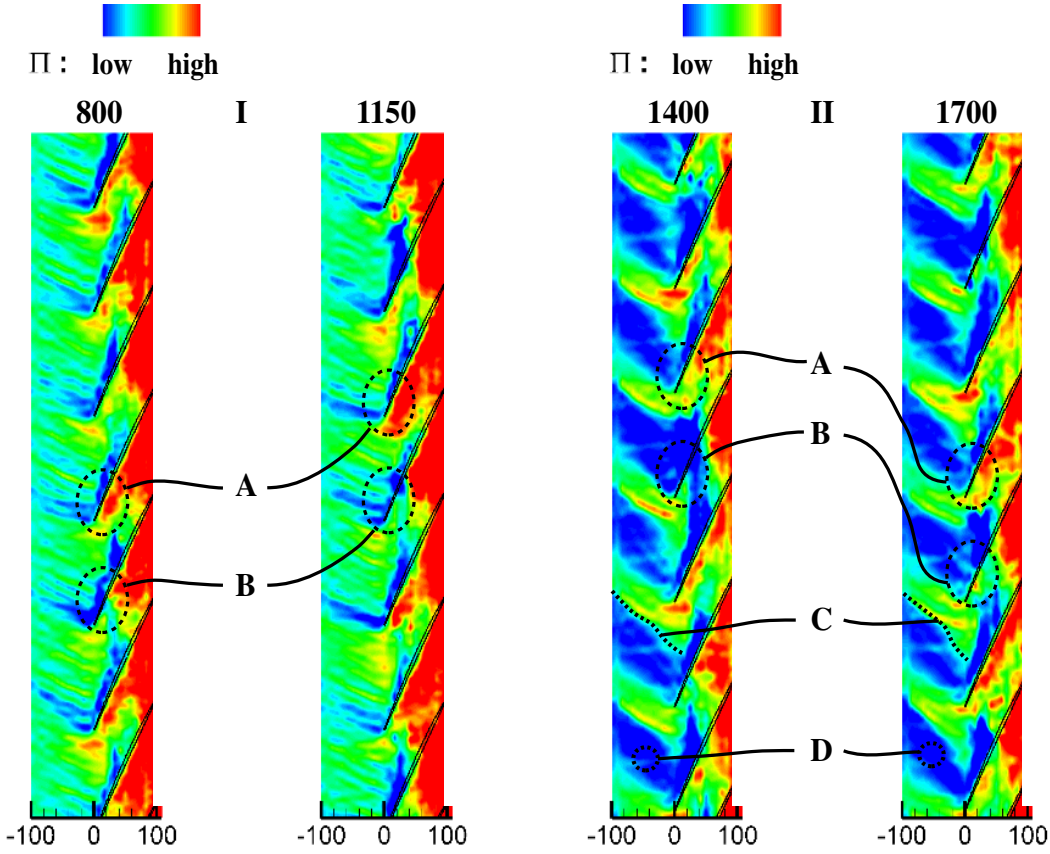

Figure 6: Unsteady pressure field at the casing wall, pressure field shown from 100% axial chord upstream of LE to 108% downstream — Measurement I, Revolution 800 and 1150 — Measurement II, Revolution 1400 and 1700 — A: High pressure gradient across blade tip — B: Low pressure gradient across blade tip — C: Position of shock — D: Expansion region

at every grid point is calculated in relation to the total pressure of the settling chamber $p_{\mathrm{t,inlet}}$ and therefore plotted as pressure ratio Π. Note that the shown image is pseudo spatial, which means that it is a snapshot of the pressure field at the time when the pressure transducer is passed.
Overall, the plots are dominated in axial direction by the pressure rise across the rotor. This is a big difference compared to measurements during which the compressor stalls. The flow field is then dominated by the stall cell (see Leichtfuss et al. [2013]). When comparing the blades in circumferential direction, it is obvious that the blades experience high and low pressure fluctuations on the PS near LE. Accordingly, the blades experience high and low pressure gradients across the blade tip, which is marked with regions A and B. This will influence the strength of the tip clearance flow and vortex and lead to alternating interactions. These interactions can build up periodical as seen and reported by Mailach et al. [2001b].
For transonic operation conditions a large expansion region D on the suction side of the blade is visible which is bordered by a final shock C (Measurement II, revolution 1400 and 1700, Figure 7). Still, the pressure fluctuations (region A and B) are visible which lead to the alternating blade loading on the PS of the blades.
The unsteady pressure fields give an impression of the flow, but it is not possible to draw definite conclusions. By computing the relative standard deviation, unsteady flow and pressure fluctuations can be estimated. Therefore, the pressure field is studied using mean and standard deviation values.

Flow Study - Mean Pressure and Standard Deviation Study Both values are calculated at every point of the measured grid. The mean pressure value $\bar{p}_s$ is related to the total pressure of the settling chamber $p_{t,inlet}$ and on this account plotted as pressure ratio Π_{mean}. The standard deviation is related to the mean pressure at every grid point:

$$\sigma_{rel} = \frac{1}{\bar{p}_s}\sqrt{\frac{1}{N-1}\sum_{k=1}^{N}(p_{s,k} - \bar{p}_s)^2} \tag{2}$$

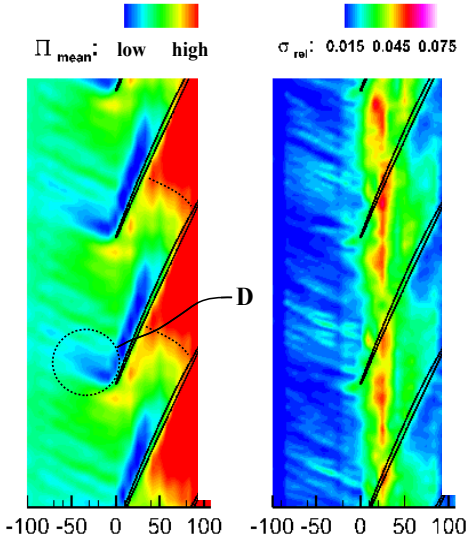

(a) Measurement I: Revolution 750 to 850

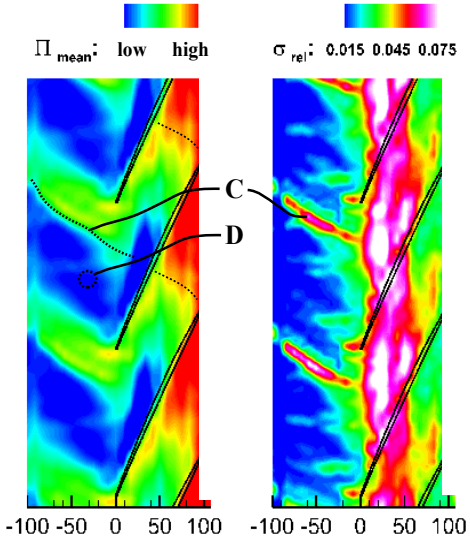

(b) Measurement II: Revolution 1300 to 1490

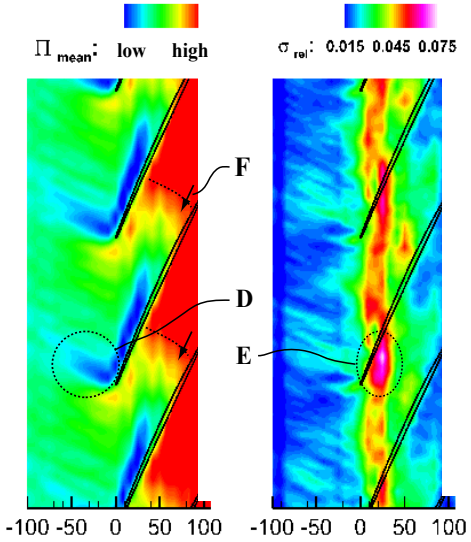

(c) Measurement I: Revolution 1100 to 1200

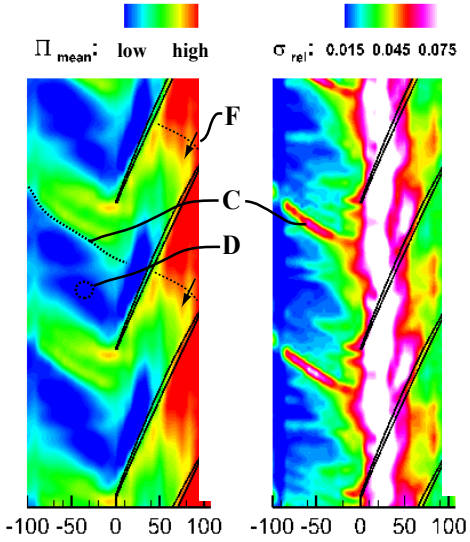

(d) Measurement II: Revolution 1675 to 1860

Figure 7: Mean pressure field and relative standard deviation of the pressure at the casing wall, pressure field shown from 100% axial chord upstream of LE to 108% downstream — C: Position of shock (Π_{mean}) and shock oscillation (σ_{rel}) — D: Expansion Region — E: Highest pressure fluctuations on PS near LE (25%) — F: Shift of the pressure region (indication remains at the same location in the blade pitch for the measurements respectively)

Usually, ensembles of 700 to 1000 revolutions of steady measurements are taken to minimize stochastic variations of the measured flow field as used by Biela [2012]. Since the analysed measurements in the present paper are transient, only 100 revolutions are used to calculate time depended results. When comparing different parts of a transient measurement it is thus possible to identify tendencies over the measurement.
After this calculation, a small expansion region D due to accelerated flow is visible on the SS of the blades in the mean pressure field of Measurement I (see Figure 7a). Between the chosen revolutions of Measurement I (revolutions 750 to 850 for Figure 7a and revolutions 1100 to 1200 for Figure 7c), only small differences in the mean pressure field are detectable. As a result of the throttle closing the high pressure region is shifted towards the LE (see indication F). In particular the fluctuations grow considerably, when comparing the relative standard deviation of the chosen revolutions. The highest fluctuations occur at approximately 25% axial chord during both parts of the measurement. Between revolution 1100 and 1200 the highest levels are clearly visible at the PS of the blades (see region E, Figure 7c), where we also noted the alternating blade loading (see Figure 6) and which is also the region of dominant blade motion for blade mode 4. The transonic case shown in Figure 7b and 7d adds to this picture. The fluctuations grow massively at 25% axial chord, when comparing the relative standard deviation between the shown revolutions. The shock position and oscillation seem to play a minor role in the analysed aeroelastic mechanism (both indicated by region C). Also, the pressure fluctuations upstream of the rotor are small, which underlines the fact, that the excitation of the vibration develops from the rotor blade row of the compressor. Especially, fluctuations are high in the region where the tip clearance vortex is located.
Consequently, it is promising to further investigate the associated frequencies of the fluctuations in the blade pitch to distinguish between random fluctuations and blade mode relevant frequencies.

Flow Study - Spectral Flow Analysis To investigate the frequencies of the pressure fluctuations in the blade pitch, the Kulite data has to be restructured. It is necessary to identify the rotor blade pitches from a given set of revolutions. Afterwards, an analysis in the frequency domain can be performed at every grid point of a blade pitch. Therefore, a spectrogram is calculated using the pressure values always at the same coordinate in subsequent blade pitches. For one spectrogram calculation 50 revolutions are taken, which computes to a frequency resolution of 5 Hz. The sampling frequency is reduced due to the fact that only one sample per pitch is taken for analysis and thus the frequencies of the fluctuations in the blade pitch are resolved only up to EO 10.5. The developed computation algorithm searches the highest amplitude in a specified range of frequencies $\mathrm{A}_{\mathrm{max}}(\Delta f)$. For both measurements the analysed frequencies range from EO 6 to EO 10.5, since these include the RI frequency band (see Figure 5). Moreover, the same revolutions are chosen as before for this investigation.
It is stated before, that the fluctuations grow considerably between the revolutions during one measurement. The spectral analysis shows, that the frequency amplitudes of the RI also rise from revolution 800 to 1150 (Figure 8a) and 1400 to 1700 (Figure 8b) respectively. Furthermore the spectral analysis of the RI frequencies verifies that these occur at the position of the highest pressure fluctuations estimated with the relative standard deviation (25% axial chord), where the tip clearance vortex is located. This clearly indicates the involvement of the blade tip vortex. The spectral analysis also underlines, that the shock does not oscillate with the frequencies of interest and is thus not a driving feature of the investigated mechanism.
Accordingly the tip clearance vortex is of high interest. It was experimentally investigated by Bae et al. [2004] using a cascade. Reduced frequencies of the pressure fluctuations in the blade passage were found to lie between 0.6 and 1.0. Using

$$F^{+} = \frac{f_{\mathrm{RI}} \cdot C}{U_{\infty}}, \tag{3}$$

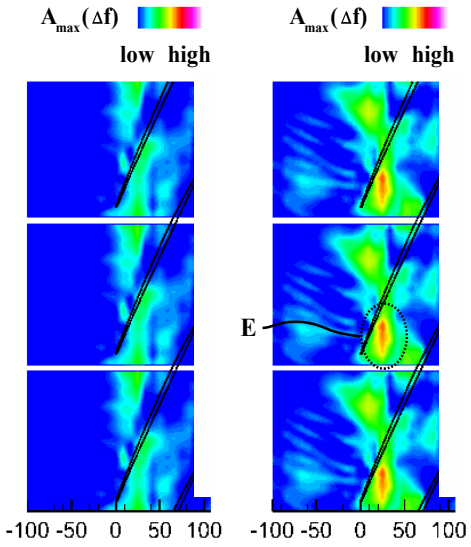

(a) Measurement I — Revolution 800 (left) and 1150 (right)

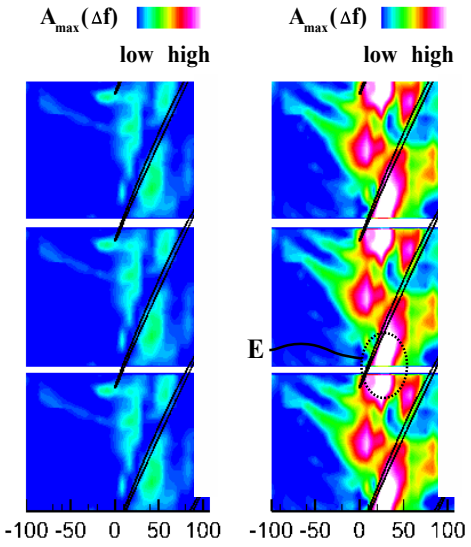

(b) Measurement II — Revolution 1400 (left) and 1700 (right)

Figure 8: Highest amplitudes in the specified range of frequencies, pressure field shown from 100% axial chord upstream of LE to 108% downstream — E: Highest pressure fluctuations on PS near LE (25%)

the reduced frequency of Measurement I computes to 1.01 and 0.88 for Measurement II. The values are computed using the incoming relative flow velocity at midspan (CFD calculation) and the measured fluctuation frequency of the RI in its own frame of reference.

Furthermore Bae et al. [2004] showed that there exists a natural frequency at which the tip clearance is most receptive to external forcing. This can explain the fact that the pressure fluctuation is enforced, when the vibration of the blade and the frequency of the pressure fluctuation synchronize (see Figure 5: Measurement I and especially Measurement II).
In particular the highest amplitudes are visible close to the PS of the blades, which matches the observations in Figure 7c. Consequently it can be concluded that the blades are excited by the RI at 0 to 25% axial chord, analogously at subsonic and transonic operation conditions.

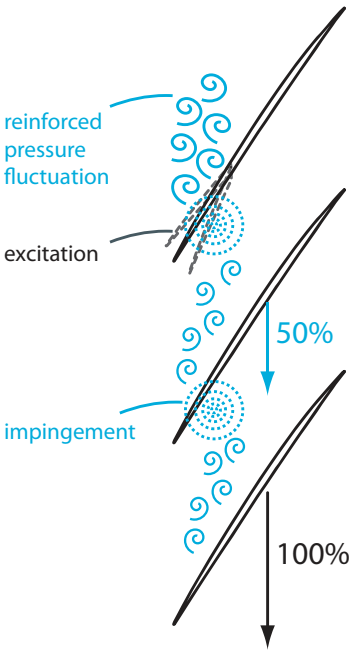

Figure 9: Sketch of the identified aeroelastic mechanism

SUMMARY AND CONCLUSIONS

This paper presents the analysis of non-synchronous vibrations for a BLISK rotor tested in the Darmstadt Transonic Compressor. Two transient measurements of a setup with an enlarged tip gap are investigated. Figure 9 sums up the identified aeroelastic mechanism. Due to the enlarged tip gap pressure fluctuations occur that rotate relative to the rotor with half of the rotor speed. This flow phenomenon is reported as rotating instability by several authors. The highest amplitudes of the pressure fluctuations are observed in the region of the tip clearance vortex. The vortex impinges at the PS of the blades and excites

the blades when the frequency matches and the aerodynamic and structural modes synchronize. The blade vibration then reinforces the pressure fluctuations in the blade pitch. Further key conclusions are:

1. A lock-on between the flow phenomenon rotating instability and the blade vibration emerges in subsonic and transonic operating conditions.
2. The frequency of the pressure fluctuations changes due to compressor throttling.
3. The blade vibrates in a broadband range of approximately 16% of the first blade mode around blade mode 4 as a result of the frequency change of the pressure fluctuation.
4. The nodal diameter changes from 1 to 0 and from 5 to 4 during the measurements respectively, when throttling the compressor. This results from the synchronization of the aerodynamic and structural frequency and circumferential mode.
5. A fluid-structure-interaction is observed, since for lock-on conditions other aerodynamic modes vanish except one which is self-excited (pressure fluctuations are reinforced).
6. Pressure fluctuations at the PS of the blades occur periodically, whereby the blade experiences low and high pressure gradients across at the blade tip causing alternating blade loading.
7. The pressure fluctuations can be matched to the frequencies of the rotating instability and the fluctuation of the tip clearance vortex.
8. At 0 to 25% axial chord the highest amplitudes are observed. The blades are excited at this axial location of the blade pitch.

ACKNOWLEDGEMENTS

The authors would like to thank *Rolls Royce Deutschland* for co-financing of the measurement campaign within the project *AGTurbo2020* and the permission to publish this work.

REFERENCES

C. Andersson, H. Martensson, and N. Edin. Non-synchronous vibrations in the $3\frac{1}{2}$ stage transonic test compressor blenda. In *The 21st International Symposium on Airbreathing Engines (ISABE)*, Busan, Korea, 2013.

J. Bae, K. S. Breuer, and C. S. Tan. Periodic unsteadiness of compressor tip clearance vortex. In *Proceedings of ASME Turbo Expo 2004: Power for Land, Sea and Air*, Vienna, Austria, June 14-17, 2004.

M. Baumgartner, F. Kameier, and J. Hourmouziadis. Non-engine order blade vibration in a high pressure compressor. In *Proceedings of 12th International Symposium on Airbreathing Engines (ISABE)*, Melbourne, Australia, September 10-15, 1995.

C. Biela. *Experimental Investigation of the Aerodynamic Influence of Inlet-Guide-Vanes on the Flow Features of a One-And-A-Half Stage Axial Transonic Compressor*. PhD thesis, Technische Universität Darmstadt, Germany, 2012.

J. D. Gill and V. R. Capace. Experimental investigation of flutter in a single stage unshrouded axial-flow fan. In *42nd AIAA Aerospace Sciences Meeting and Exhibit*, Reno, Nevada, 5 - 8 January 2004.

F. Kameier and W. Neise. Rotating blade flow instability as a source of noise in axial turbomachines. *Journal of Sound and Vibration*, 203(5):833–853, 1997.

R. E. Kielb, J. W. Barter, J. P. Thomas, and K. C. Hall. Blade excitation by aerodynamic instabilities: A compressor blade study. In *Proceedings of the ASME Turbo Expo 2003: Power for Land, Sea, and Air*, Atlanta, Georgia, USA, June 16–19 2003.

S. Leichtfuss, F. Holzinger, C. Brandstetter, F. Wartzek, and H. P. Schiffer. Aeroelastic investigation

of a transonic research compressor. In *Proceedings of the ASME Turbo Expo 2013: Power for Land, Sea and Air*, San Antonio, Texas, June 03-07, 2013.

R. Mailach, I. Lehmann, and K. Vogeler. Rotating instabilities in an axial compressor originating from the fluctuating blade tip vortex. *Journal of Turbomachinery*, 123(3):453–460, 2001a.

R. Mailach, H. Sauer, and K. Vogeler. The periodical interaction of the tip clearance flow in the blade rows of axial compressors. In *Proceedings of the 46th ASME Turbo Expo*, New Orleans, Louisiana, USA, June 4-7 2001b.

H. Martensson, C. Andersson, and N. Edin. Aeroelastic instability of antransonic compressor near stall. In *13th International Symposium on Unsteady Aerodynamics, Aeroacoustics and Aeroelasticity of Turbomachines (ISUAAAT) 2012*, Tokyo, Japan, 11-14 September 2012.

J. März, C. Hah, and W. Neise. An experimental and numerical investigation into the mechanisms of rotating instability. *Journal of Turbomachinery*, 124(3):367–374, 2002.

F. Sisto. Introduction and overview. In *AGARD Manual on Aeroelasticity 1988*, volume AGARD-AG-298-VOL-2, pages 12–1/12–2. 1988.

Srinivasan, A. V. Flutter and resonant vibration characteristics of engine blades. In *Proceedings of the 1997 International Gas Turbine & Aeroengine Congress & Exposition*, Orlando, FL, USA, 2-5 June 1997.

H. D. Vo. Role of tip clearance flow in the generation of non-synchronous vibrations. In *44th AIAA Aerospace,sciences Meeting and Exhibit*, Reno, Nevada, 9-12 January 2006.

M. Zielinski and G. Ziller. Noncontact vibration measurements on compressor rotor blades. *Measurement Science and Technology*, 11(7):847–856, 2000.